

On achievable accuracy for range-finder localization

Andrea Censi

Università degli Studi di Roma “La Sapienza”
 Dipartimento di Informatica e Sistemistica “A. Ruberti”
 via Eudossiana 18, I-00184 Rome, Italy
 andrea.censi@dis.uniroma1.it

Abstract—The covariance of every unbiased estimator is bounded by the Cramér–Rao lower bound, which is the inverse of Fisher’s information matrix. This paper shows that, for the case of localization with range-finders, Fisher’s matrix is a function of the expected readings and of the orientation of the environment’s surfaces at the sensed points. The matrix also offers a mathematically sound way to characterize under-constrained situations as those for which it is singular: in those cases the kernel describes the direction of maximum uncertainty. This paper also introduces a simple model of unstructured environments for which the Cramér–Rao bound is a function of two statistics of the shape of the environment: the average radius and a measure of the irregularity of the surfaces. Although this model is not valid for all environments, it allows for some interesting qualitative considerations. As an experimental validation, this paper reports simulations comparing the bound with the actual performance of the ICP (Iterative Closest/Corresponding Point) algorithm. Finally, it is discussed the difficulty in extending these results to find a lower bound for accuracy in scan matching and SLAM.

I. INTRODUCTION

This paper describes a theoretical limit to the precision of localization methods employing range-finder data. Most of the current methods model localization as a state estimation problem: the state is the robot’s pose \mathbf{x} and the sensor data is modelled as a random variable \mathbf{z} . Once in the probabilistic framework, a localization algorithm is an estimator of \mathbf{x} given \mathbf{z} . The problem can be analyzed using classical tools of mathematical statistics, establishing the Cramér–Rao lower bound (CRB) for the covariance of unbiased estimators of \mathbf{x} .

The CRB provides a *quantitative* reference for comparing the performance of actual algorithms, which are often hard to analyze mathematically: the example of the ICP (Iterative Closest/Corresponding Point) will be discussed as an example. The CRB is valid, but weak, for scan matching (recovering the robot’s displacement by comparing two successive sensor scans), the reason being that the uncertainty of the map is not modelled here; however, it will be shown that it gives an indication of the directions with more uncertainty.

The CRB also allows for a *qualitative* analysis of localization. Under-constrained situations are those in which Fisher’s matrix is singular: therefore it is possible to perform an accurate observability analysis of the problem [1]. This paper also presents a qualitative model for unstructured environments that shows how the environment size, the shape, and the sensor noise contribute to the achievable accuracy bound.

TABLE I
 SYMBOLS USED IN THIS PAPER

Statistics	
\mathbf{x}	Quantity to estimate.
\mathbf{z}	Available measurements.
$\hat{\mathbf{x}} = A(\mathbf{z})$	An estimate of \mathbf{x} obtained using algorithm A on the data \mathbf{z} .
$E_z\{f(\mathbf{z})\}$	Expectation operation with respect to the density of \mathbf{z} . $E_z\{f(\mathbf{z})\} \triangleq \int f(\mathbf{z})p(\mathbf{z})d\mathbf{z}$
$\mathcal{I}(\mathbf{x})$	Fisher’s information matrix.
Localization	
$\mathbf{x} = (t, \theta)$	The robot/sensor pose.
n	Number of rays.
$\mathbf{z} = \{\tilde{\rho}_i\}$	Output of range-finder. $i = 1 \dots n$
φ_i	Casting direction for i -th ray.
$\tilde{\rho}_i$	Measurement along direction φ_i .
$r(\mathbf{p}, \phi)$	“ray-tracing function”: the distance from point \mathbf{p} to the nearest obstacle in the ϕ direction.
α_i	Surface orientation at the sensed point.
Δ	Angle interval, assuming equally spaced rays.
FOV	Sensor’s field of view (FOV = $n \cdot \Delta$).
r_i	$\triangleq r(\mathbf{t}, \theta + \varphi_i)$
\mathbf{v}_i	$\triangleq \mathbf{v}(\theta + \varphi_i)$
Miscellaneous	
$a, \mathbf{a}, \mathbf{A}$	Scalar, vectorial, matrix quantity.
$\partial f / \partial \mathbf{x}$	Row vector, defined as $(\partial f / \partial x_1 \dots \partial f / \partial x_n)$ for $\mathbf{x} \in \mathbb{R}^n$ and $f : \mathbb{R}^n \rightarrow \mathbb{R}$.
$\mathbf{R}(\varphi)$	2×2 rotation matrix.
$\mathbf{v}(a)$	Column vector, defined as $(\cos a \quad \sin a)^T$.
$\hat{\mathbf{a}}$	Column vector, defined as $\mathbf{R}(\pi/2)\mathbf{a}$.

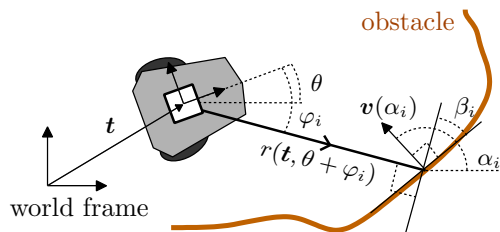


Fig. 1. The robot coordinates are $\mathbf{x} = (t, \theta)$ with respect to a fixed world frame. The i -th sensor ray is cast in direction φ_i . The actual distance of the sensed obstacle is $r(t, \theta + \varphi_i)$. The angle α_i is the direction of the normal to the curve and the vector $\mathbf{v}(\alpha_i)$ is its corresponding versor.

II. THE CRB FOR RANGE-FINDER LOCALIZATION

Consider a robot equipped with a range-finder in a planar environment. Let the robot's pose be $\mathbf{x} \triangleq (\mathbf{t}, \theta)$ with respect to a fixed world frame and, without loss of generality, let the sensor frame be coincident with the robot's frame.

Assume the output of the sensor to be a set \mathbf{z} of n range measurements, with $\tilde{\rho}_i$ being the range measurement for the i -th ray along direction φ_i . Define the "ray tracing function" $r : \mathbb{R}^2 \times [0, 2\pi) \rightarrow \mathbb{R}^+$ such that $r(\mathbf{p}, \psi)$ is the distance from point \mathbf{p} to the nearest obstacle in direction ψ . The function r completely defines the environment. With this notation, the sensor model is

$$\tilde{\rho}_i = r(\mathbf{t}, \theta + \varphi_i) + \epsilon_i \quad i = 1 \dots n \quad (1)$$

The term ϵ_i is assumed to be a Gaussian random variable with zero mean and variance σ^2 . This model ignores the bias term on $\tilde{\rho}_i$ which is specific to the device and is a function of distance, orientation, color, and material of the surface [2]; in high-speed robotics [3] also the motion of the robot while sensing might introduce a non-negligible bias.

Fisher's information matrix is defined by the first derivatives of the ray-tracing function r with respect to \mathbf{t} and θ — a step by step derivation is given in section A of the Appendix.

$$\mathcal{I}(\mathbf{x}) = \frac{1}{\sigma^2} \sum_i^n \begin{bmatrix} \frac{\partial r_i}{\partial \mathbf{x}} & \frac{\partial r_i}{\partial \theta} \end{bmatrix} \quad r_i \triangleq r(\mathbf{t}, \theta + \varphi_i) \quad (2)$$

The necessary derivatives depend on the surface's orientation α at the point intercepted by each ray (Fig. 1)¹.

$$\frac{\partial r(\mathbf{t}, \theta + \varphi_i)}{\partial \theta} = r(\mathbf{t}, \theta + \varphi_i) \tan(\beta_i) \quad (3)$$

$$\frac{\partial r(\mathbf{t}, \theta + \varphi_i)}{\partial \mathbf{t}} = \mathbf{v}(\alpha_i) / \cos(\beta_i) \quad (4)$$

where $\beta_i \triangleq \alpha_i - (\theta + \varphi_i)$. By substituting (3), (4) in (2):

$$\mathcal{I}(\mathbf{x}) = \frac{1}{\sigma^2} \sum_i^n \begin{bmatrix} \frac{\mathbf{v}(\alpha_i)\mathbf{v}(\alpha_i)^\top}{\cos^2 \beta_i} & r_i \frac{\tan \beta_i}{\cos \beta_i} \mathbf{v}(\alpha_i) \\ * & r_i^2 \tan^2 \beta_i \end{bmatrix} \quad (5)$$

The achievable error covariance is given by the inverse of $\mathcal{I}(\mathbf{x})$. These formulas are valid for every disposition of the rays and for every environment. The results are not intuitive at all: see Fig. 2 for some examples.

The CRB is attainable only if r is a (locally) linear function of its arguments [4]: that is, successive derivatives are zero at the considered point. This is possible for \mathbf{t} in a polygonal environment where $\partial r / \partial \mathbf{t}$ is locally constant and the bound is attainable. As for θ , the function $r(\cdot, \mathbf{t})$ is non-linear, therefore the bound is not tight. However, in practice (see Section IV), the CRB is very close to the accuracy achieved by actual algorithms.

Under-constrained situations: Fisher's information matrix allows for characterizing under-constrained situations are

¹The Cramér–Rao bound is not defined where $r(\mathbf{t}, \theta + \varphi_i)$ is not continuous (condition (11)): this happens when the sensor point samples exactly the edge of one of the surfaces in the environment: in that case a small variation of \mathbf{x} makes r 'jump'. Note however that the set of \mathbf{x} such that r is not continuous is a set of measure 0.

"LOCALIZABILITY" IN A SQUARE ENVIRONMENT

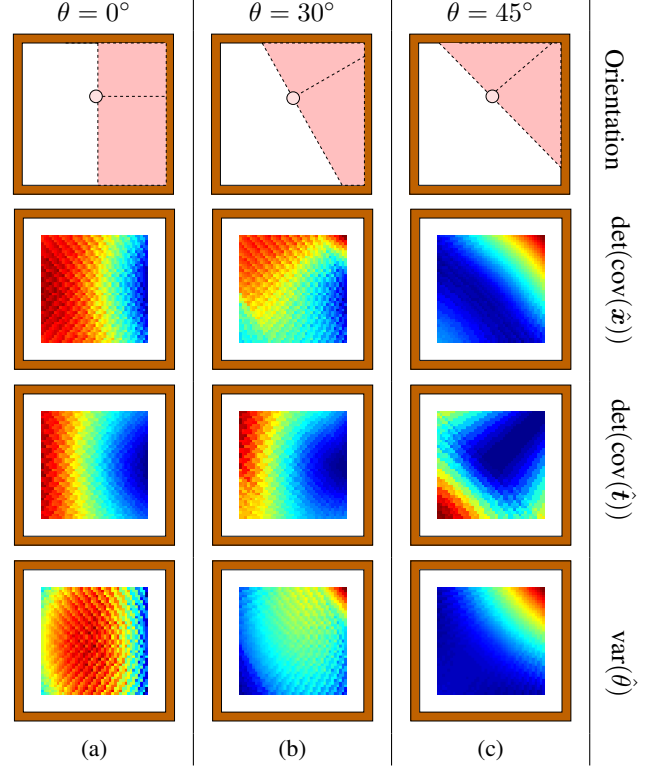


Fig. 2. Each column shows the results with a different orientation of the robot. In each image, the orientation θ is kept fixed, while x and y change at each pixel. Three statistics are displayed: the determinant of $\text{cov}(\hat{\mathbf{x}})$ that is a measure of the global achievable accuracy, the determinant of $\text{cov}(\hat{\mathbf{t}})$ and the variance of θ . Red areas denote large values, which mean low achievable accuracy, while blue areas correspond to high accuracy.

KERNEL OF THE INFORMATION MATRIX IN A CIRCULAR ENVIRONMENT

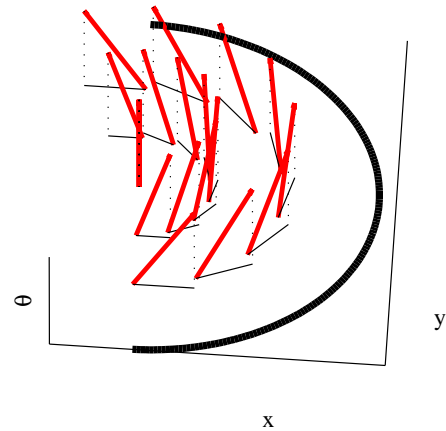


Fig. 3. In a circular environment the information matrix has a null eigenvalue. This figure shows the corresponding eigenvectors in the x, y, θ space as thick red segments. The thin black segments are the projections of such eigenvectors on the x, y plane. At the center of the circle the uncertainty is concentrated only on θ ; when the robot is near the walls, the estimate of θ becomes correlated with the estimate of \mathbf{t} . Intuitively, at the center the robot might rotate and continue to get the same readings; in the other places it has to rotate *and* translate to obtain the same effect.

those for which it is singular. Eigenvectors of $\mathcal{I}(\mathbf{x})$ corresponding to small eigenvalues are the directions (in the x, y, θ space) of maximum uncertainty.

There are two such situations: if all the surfaces are locally parallel (e.g. corridor) or if they are all concentric; in both cases it is possible to give a closed-form expression for the eigenvectors (see the Appendix for a proof). For example, in a corridor with no end the kernel of $\mathcal{I}(\mathbf{x})$ is along the corridor direction. Similarly, in a circular environment there is a null eigenvalue, whose eigenvector changes according to the pose of the robot (Fig. 3).

III. A MODEL FOR UNSTRUCTURED ENVIRONMENTS

In this section a “generic” unstructured environment is considered and it is shown that, under appropriate assumptions, the CRB is a function of two simple statistics of the shape of the environment: the average radius and a measure of the irregularity of the shape. This allows for a number of interesting qualitative considerations.

Consider a robot at the center of an approximately circular environment (Fig. 4) with average radius $\bar{\rho}$, described by the ray-tracing function as:

$$r(\mathbf{0}, \phi) = \bar{\rho} + f(\phi \bar{\rho}) \quad |f| \ll \bar{\rho} \quad (6)$$

The function f is assumed to be periodic with period $2\pi\bar{\rho}$ and continuously derivable.

Proposition 1: If $f(s)$ is a realization of a random process which is stationary and ergodic with respect to s , then, by indicating with $E_f\{\cdot\}$ the expectation with respect to the possible realizations of f , the expectation of the information matrix at the center can be expressed as a function of $\bar{\rho}$ and $\mathcal{C} \triangleq E_f\{f'^2\}$.

In the case of a 180° sensor:

$$E_f\{\mathcal{I}(\mathbf{0}, \theta)\} \simeq \frac{n}{\sigma^2} \begin{bmatrix} \frac{1+\mathcal{C}}{2} \mathbf{I}_{2 \times 2} & \mathbf{R}(\theta) \begin{bmatrix} 0 \\ 2\rho\mathcal{C}/\pi \end{bmatrix} \\ * & \bar{\rho}^2 \mathcal{C} \end{bmatrix} \quad (7)$$

For a 360° sensor:

$$E_f\{\mathcal{I}(\mathbf{0}, \theta)\} \simeq \frac{n}{\sigma^2} \begin{bmatrix} \frac{1+\mathcal{C}}{2} \mathbf{I}_{2 \times 2} & \begin{bmatrix} 0 \\ 0 \end{bmatrix} \\ * & \bar{\rho}^2 \mathcal{C} \end{bmatrix} \quad (8)$$

The approximation is valid if the sampling is dense with respect to the bandwidth of f . (See the Appendix for a proof).

It is possible to express some intuitive considerations based on Proposition 1. Note that for a 360° sensor, (8) is block diagonal: there is “on average” no correlation between θ and t , while for a 180° sensor a correlation exists. Moreover, from (8) it follows that, for any unbiased estimator $(\hat{t}, \hat{\theta})$, in an “average” unstructured environment,

$$\text{var}(\hat{\theta}) \geq \frac{(\sigma/\bar{\rho})^2}{n} \frac{1}{\mathcal{C}} \quad (9)$$

$$\lambda_{\min \text{cov}}(\hat{\mathbf{t}}) \geq 2 \frac{\sigma^2}{n} \frac{1}{1+\mathcal{C}} \quad (10)$$

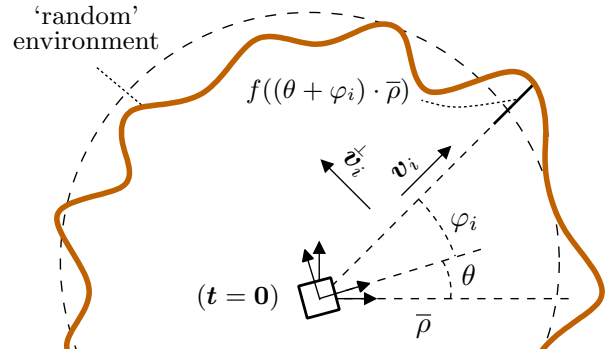


Fig. 4. A simple model for unstructured environments. The robot is assumed to be at the center of an approximately circular environment: the average radius is $\bar{\rho}$ and the function f describes the profile of the environment. For this environment, Fisher’s information matrix is a function of the radius and of $\mathcal{C} \triangleq E_f\{f'^2\}$.

- If $\mathcal{C} \rightarrow 0$, then $f' \rightarrow 0$ and the environment tends to a circle. For a circle, the uncertainty on θ is infinite, while the uncertainty for t is still finite.
- For both θ and t , high values of \mathcal{C} correspond to low values of the covariance: intuitively, localization is easier if the environment is irregular, jagged and rich in features.
- The accuracy for θ depends on the “normalized” noise deviation $\sigma/\bar{\rho}$. This expresses an invariance to scale: in a bigger environment the bound is constant if the noise is scaled accordingly; in other words, for θ , it is the shape that matters, not the size.

IV. SIMULATIONS

The goal of the experiments was to compare the covariance of the error of an actual algorithm with the CRB, and to see how weak is the bound for scan matching. Experiments have been performed in a simulated environment because a very precise ground-truth (sub-millimeter accuracy) is needed.

The algorithm used is the ICP [5] because it is simple, popular, and many researchers have a first-hand experience with it. Although many variants exist, and special particularizations to robot localization have been investigated, the ‘vanilla’ version was employed (point-to-point distance, linear interpolation in the reference scan). Results were found consistent among a series of different environments; the simple square environment is used here for ease of reproducibility.

Some caveats: for the CRB to hold exactly, two conditions should be met: (a) “localization” is performed, that is, the world is perfectly known, and (b) the algorithm is unbiased. To achieve (a), the reference scan was set as a zero-noise dense sampling of the environment: in such a way the environment is effectively “known” to the ICP. To achieve (b), the trials were performed in a situation of perfect symmetry: at the center of a square environment with a 360° sensor. Another series of experiments was performed, with a 180° scan taken at $\mathbf{x} = (-2m, 2m, 30^\circ)$. Sometimes ([6],

[7]) performance benchmarks are executed by changing only the starting guess, without simulating the sensor noise: that originates a characteristic cluster-like distribution of errors. Conversely, if one simulates sensor noise, then a familiar and reassuring ellipsoidal distribution appears.

In all experiments, an excellent match of the ICP covariance with the CRB was observed (Fig. 5). In the symmetric case, the three components of \mathbf{x} are uncorrelated. In the asymmetric case, there is a correlation between x and θ which is perfectly predicted by the CRB. Another series of experiments was performed to simulate scan matching, by matching pairs of noisy scans. The bound is indeed weak for scan matching, but still it gives an approximation of the directions with more uncertainty.

V. CONCLUSIONS AND FUTURE WORK

This paper refers only to localization. The CRB is valid but weak for scan matching or SLAM; the reason being that the dominant uncertainty in those problems is the uncertainty of the map, which is not modelled here. It is the author's opinion that this line of research, should it be possible to be extended to SLAM, might allow for obtaining convergence results or quality guarantees for SLAM methods employing raw laser data: consider as an example Rao–Blackwellized particle filters [8], which have recently provided impressive results but really lack adequate theoretical analysis (this is a general problem for particle filters [9]).

Before approaching SLAM, one should consider the problem of *mapping*, that is estimating a model of the environment given scans taken at known positions. Bounds for mapping are harder to define because the problem is infinite-dimensional. In neighboring fields there are problems conceptually similar to mapping, however the results seem to be not easily transferable. Many localization algorithms have been borrowed from the vision community which uses range-finders. One typical application is to reconstruct the shape of an object through dense three-dimensional scans; it is important to assess the accuracy of the reconstruction (e.g. for forensics analysis). [10] studies the CRB for surface reconstruction from multiple scans, but the hypothesis assumed (that the resolution is so high so that different scans sample exactly the same points) makes that result not applicable to robotic mapping. Cramér–Rao bounds have been studied also for functional inverse problems: for example for the problem of passive radar imaging [11] and tomography [12], [13], but the results do not seem to be applicable to mapping.

Nevertheless, what we can understand from these works is that the key for a good analysis is to choose a good representation, possibly finite-dimensional. For example, a polygonal environment has a finite-dimensional representation for which it is very easy to define the CRB given range measurements. Other candidate representations include splines or Gaussian processes [14] for which it is possible to define some kind of prior over the possible worlds and inference is not difficult, as opposed, for example, to Elfes' occupancy grids [15] for which inference is tricky due to the cell-independence assumption.

Future work will concern investigating such representations for use in robotic mapping.

APPENDIX

A. The Cramér–Rao inequality

Let $\mathbf{x} \in \mathbb{R}^q$ be an unknown, fixed quantity to be estimated through the measurements $\mathbf{z} \in \mathbb{R}^n$, affected by noise and modelled as a random variable.

Cramér–Rao inequality. *If the density $p(\mathbf{z}, \mathbf{x})$ satisfies two regularity conditions:*

- 1) *The derivative of the log-likelihood function is finite*

$$\frac{\partial \log p(\mathbf{z}, \mathbf{x})}{\partial \mathbf{x}} < \infty \quad \forall \mathbf{x} : p(\mathbf{z}, \mathbf{x}) > 0 \quad (11)$$

- 2) *For any finite statistic $T(\mathbf{z})$ such that $E_{\mathbf{z}}\{T(\mathbf{z})\} < \infty$ the operation of integration with respect to \mathbf{z} and derivation with respect to \mathbf{x} can be interchanged in $\int T(\mathbf{z})p(\mathbf{z}, \mathbf{x})d\mathbf{z}$:*

$$\frac{\partial}{\partial \mathbf{x}} \int T(\mathbf{z})p(\mathbf{z}, \mathbf{x})d\mathbf{z} = \int T(\mathbf{z}) \frac{\partial}{\partial \mathbf{x}} p(\mathbf{z}, \mathbf{x})d\mathbf{z} \quad (12)$$

Then for any unbiased estimator $\hat{\mathbf{x}}$,

$$\text{cov}(\hat{\mathbf{x}}) \geq [\mathcal{I}(\mathbf{x})]^{-1} \quad (13)$$

The $q \times q$ symmetric matrix $\mathcal{I}(\mathbf{x})$, called Fisher's information matrix, is defined as

$$\mathcal{I}(\mathbf{x}) = E_{\mathbf{z}} \left\{ \frac{\partial \log p(\mathbf{z}, \mathbf{x})}{\partial \mathbf{x}} \frac{\partial \log p(\mathbf{z}, \mathbf{x})}{\partial \mathbf{x}}^T \right\} \quad (14)$$

In the Gaussian case, the bound has a simple form. Consider the observation model described in (1). Compute the derivative of the log-density: $\partial(\log p)/\partial \mathbf{x} = -\sum_i (\epsilon_i/\sigma^2) \partial r_i / \partial \mathbf{x}$. The information matrix contains the expectation of the product of two sums:

$$\mathcal{I}(\mathbf{x}) = E_{\mathbf{z}} \left\{ \sum_i^n -\frac{\epsilon_i}{\sigma^2} \frac{\partial r_i}{\partial \mathbf{x}}^T \sum_j^n -\frac{\epsilon_j}{\sigma^2} \frac{\partial r_j}{\partial \mathbf{x}} \right\} \quad (15)$$

Expand the sums to highlight the mixed products:

$$\mathcal{I}(\mathbf{x}) = \sum_i^n \frac{E_{\mathbf{z}}\{\epsilon_i^2\}}{\sigma^4} \frac{\partial r_i^T}{\partial \mathbf{x}} \frac{\partial r_i}{\partial \mathbf{x}} + \sum_i^n \sum_{j \neq i}^n \frac{E_{\mathbf{z}}\{\epsilon_i \epsilon_j\}}{\sigma^4} \frac{\partial r_i^T}{\partial \mathbf{x}} \frac{\partial r_j}{\partial \mathbf{x}} \quad (16)$$

The term $E_{\mathbf{z}}\{\epsilon_i \epsilon_j\}$ is null because of independence, while $E_{\mathbf{z}}\{\epsilon_i^2\} = \sigma^2$. Finally one obtains (2).

B. Under-constrained situations

It will be shown that Fisher's information matrix is singular in the following cases by explicitly giving an expression for the kernel's eigenvector \mathbf{k} .

Lemma 1: Necessary and sufficient condition for \mathbf{k} to belong to the kernel of $\mathcal{I}(\mathbf{x})$ is that $\forall i (\partial r_i / \partial \mathbf{x}) \mathbf{k} = 0$.

Proof: (Sufficiency) Assume that $\forall i (\partial r_i / \partial \mathbf{x}) \mathbf{k} = 0$. Then:

$$\mathcal{I}(\mathbf{x}) \mathbf{k} = \frac{1}{\sigma^2} \sum_i^n \frac{\partial r_i^T}{\partial \mathbf{x}} \left(\frac{\partial r_i}{\partial \mathbf{x}} \mathbf{k} \right) = \frac{1}{\sigma^2} \sum_i^n \frac{\partial r_i^T}{\partial \mathbf{x}} 0 = \mathbf{0} \quad (17)$$

(Necessity) Assume that $\mathbf{k} \in \ker \mathcal{I}(\mathbf{x})$. Write $\mathcal{I}(\mathbf{x})$ as $\mathcal{I}(\mathbf{x}) = \sum_i \mathcal{I}_i(\mathbf{x})$ where $\mathcal{I}_i(\mathbf{x}) \triangleq (1/\sigma^2)(\partial r_i/\partial \mathbf{x})^\top (\partial r_i/\partial \mathbf{x})$. Note that $\mathcal{I}_i(\mathbf{x})$ is a 3×3 semi-definite positive matrix. It follows that $\mathcal{I}_i(\mathbf{x}) \leq \mathcal{I}(\mathbf{x})$ and $\ker \mathcal{I}(\mathbf{x}) \subset \ker \mathcal{I}_i(\mathbf{x})$: therefore $\mathbf{k} \in \ker \mathcal{I}_i(\mathbf{x})$. Because $(\partial r_i/\partial \mathbf{x})^\top \neq \mathbf{0}$, $\mathcal{I}_i(\mathbf{x})\mathbf{k} = 0$ implies that $(\partial r_i/\partial \mathbf{x})\mathbf{k} = 0$. ■

a) All surfaces locally parallel (e.g. corridor): $\mathbf{k} = [\dot{\mathbf{v}}(\bar{\alpha}); 0]$. Assume that every surface of the environment (at the sensed points) is parallel to each other: $\alpha_i = \bar{\alpha}$ or $\alpha_i = \bar{\alpha} + \pi$ (so that $\mathbf{v}(\alpha_i) = \pm \mathbf{v}(\bar{\alpha})$). Then, because $\mathbf{v}(\bar{\alpha})^\top \dot{\mathbf{v}}(\bar{\alpha}) = 0$,

$$\frac{\partial r_i}{\partial \mathbf{x}} \mathbf{k} = \begin{bmatrix} \pm \mathbf{v}(\bar{\alpha})^\top & r_i \tan(\beta_i) \\ \cos(\beta_i) & 0 \end{bmatrix} \begin{bmatrix} \dot{\mathbf{v}}(\bar{\alpha}) \\ 0 \end{bmatrix} = 0 \quad (18)$$

b) All surfaces locally concentric (e.g. circle); robot at center: $\mathbf{k} = [0; 0; 1]$. Consider the case in which all surfaces are arcs of circumferences whose common center is $(0, 0)$. If the robot is at the center ($\mathbf{t} = \mathbf{0}$), then $\beta_i = 0$ for all i , and

$$\frac{\partial r_i}{\partial \mathbf{x}} \mathbf{k} = \begin{bmatrix} \mathbf{v}(\alpha_i)^\top & 0 \end{bmatrix} \begin{bmatrix} \mathbf{0} \\ 1 \end{bmatrix} = 0 \quad (19)$$

c) All surfaces locally concentric; robot not at center: $\mathbf{k} = [\dot{\mathbf{t}}; 1]$. This case requires a longer proof. Consider the point \mathbf{p}_i which is the point intercepted by the sensor ray: $\mathbf{p}_i = \mathbf{t} + r_i \mathbf{v}(\theta + \varphi_i)$. Now assume that each \mathbf{p}_i lies on a circumference with center $(0, 0)$ and radius R_i : $\|\mathbf{p}_i\| = R_i$. Square both sides to obtain the implicit function $h(r_i, \mathbf{x}) = 0$ which binds r_i and \mathbf{x} (abbreviate $\mathbf{v}(\theta + \varphi_i)$ as \mathbf{v}_i):

$$h(r_i, \mathbf{x}) = (\mathbf{t} + r_i \mathbf{v}_i)^\top (\mathbf{t} + r_i \mathbf{v}_i) - R_i^2 = 0 \quad (20)$$

From the implicit function theorem it follows that $\partial r_i/\partial \mathbf{x} = (\partial h/\partial r_i)^{-1} \partial h/\partial \mathbf{x}$ provided that $(\partial h/\partial r_i) \neq 0$ (note that $\mathcal{I}(\mathbf{x})$ is not defined where $\partial r_i/\partial \mathbf{x}$ does not exist). The necessary derivatives are

$$\begin{aligned} \frac{\partial h}{\partial \mathbf{x}} &= 2 \left[\overbrace{(\mathbf{t}^\top + r_i \mathbf{v}_i^\top)}^{1 \times 3} \quad \overbrace{r_i \mathbf{t}^\top \dot{\mathbf{v}}_i}^{1 \times 1} \right] \\ \frac{\partial h}{\partial r_i} &= 2 (\mathbf{t}^\top \mathbf{v}_i + r_i) \end{aligned} \quad (21)$$

Finally it is possible to verify that $(\partial r_i/\partial \mathbf{x})\mathbf{k} = 0$:

$$\frac{\partial r_i}{\partial \mathbf{x}} \mathbf{k} \propto \frac{\partial h}{\partial \mathbf{x}} \begin{bmatrix} \dot{\mathbf{t}} \\ 1 \end{bmatrix} = 2 (\mathbf{t}^\top \dot{\mathbf{t}} + r_i \mathbf{v}_i^\top \dot{\mathbf{t}} + r_i \mathbf{t}^\top \dot{\mathbf{v}}_i) = 0 \quad (22)$$

The last passage exploited the fact that $\mathbf{a}^\top \dot{\mathbf{a}} = 0$ and that $\mathbf{a}^\top \dot{\mathbf{b}} = -\mathbf{b}^\top \dot{\mathbf{a}}$.

Note that the three cases discussed encompass all possible situations: if $\mathbf{k} = [*; *; 0]$, the environment is locally invariant to a pure translation of the robot (and therefore all surfaces are parallel); if $\mathbf{k} = [0; 0; *]$, the environment is locally invariant to a pure rotation (and therefore all surfaces are concentric); if $\mathbf{k} = [*; *; *]$ the environment is locally invariant to a roto-translation (the surfaces are concentric but the robot is not at the center).

C. Proof of Proposition 1

Partition the information matrix in four blocks:

$$E_f\{\mathcal{I}(\mathbf{x})\} \triangleq \begin{bmatrix} E_f\{\mathcal{I}(\mathbf{t})\} & E_f\{\mathcal{I}(\mathbf{t}, \theta)\} \\ * & E_f\{\mathcal{I}(\theta)\} \end{bmatrix} \quad (23)$$

The proof will be given for each block separately.

a) Derivation of $E_f\{\mathcal{I}(\theta)\}$. From (6) it follows that $\partial r_i/\partial \theta = \bar{\rho} f'_i$ and therefore $\mathcal{I}(\theta) = (\bar{\rho}^2/\sigma^2) \sum_i (f'_i)^2$. By taking the expectation one obtains $E_f\{\mathcal{I}(\theta)\} = (\bar{\rho}/\sigma)^2 \cdot n\mathcal{C}$ where $\mathcal{C} \triangleq E_f\{f_i'^2\}$.

b) Derivation of $E_f\{\mathcal{I}(\mathbf{t})\}$. An expression for $\partial r_i/\partial \mathbf{t}$ can be inferred from geometric inspection of Fig. 4. The robot is at the center: $\mathbf{t} = \mathbf{0}$. Consider $\delta \mathbf{t}$, an infinitesimal variation of \mathbf{t} along direction $\mathbf{v}_i \triangleq \mathbf{v}(\theta + \varphi_i)$ (the ray's direction): r_i becomes smaller of $|\delta \mathbf{t}|$. Instead, if $\delta \mathbf{t}$ is parallel to $\dot{\mathbf{v}}_i$, the variation of r_i depends on the angle β_i , which is related to the first derivative of f at the intercept's point ($\tan \beta_i = f'_i$). Putting all of this together:

$$\frac{\partial r_i}{\partial \mathbf{t}} = -\mathbf{v}_i^\top + (\tan \beta_i) \dot{\mathbf{v}}_i^\top = -\mathbf{v}_i^\top + (f'_i) \dot{\mathbf{v}}_i^\top \quad (24)$$

Substituting this into (14):

$$\mathcal{I}(\mathbf{t}) = \frac{1}{\sigma^2} \sum_i^n (-\mathbf{v}_i + f'_i \dot{\mathbf{v}}_i) (-\mathbf{v}_i + f'_i \dot{\mathbf{v}}_i)^\top \quad (25)$$

Expand the product and take the expectation:

$$\begin{aligned} E_f\{\mathcal{I}(\mathbf{t})\} &= \frac{1}{\sigma^2} \sum_i^n \mathbf{v}_i \mathbf{v}_i^\top + \frac{1}{\sigma^2} E_f\{f_i'^2\} \sum_i^n \dot{\mathbf{v}}_i \dot{\mathbf{v}}_i^\top + \\ &\quad + \frac{1}{\sigma^2} E_f\{f'_i\} \sum_i^n (-\dot{\mathbf{v}}_i \mathbf{v}_i^\top - \mathbf{v}_i \dot{\mathbf{v}}_i^\top) \end{aligned} \quad (26)$$

Because f is periodic and the process is ergodic, $E_f\{f'\} = 0$. For a 360° or a 180° FOV sensor with dense, equally spaced rays, the sums $\sum_i \dot{\mathbf{v}}_i \dot{\mathbf{v}}_i^\top$, $\sum_i \mathbf{v}_i \mathbf{v}_i^\top$ can be approximated with an integral; one obtains, setting $\mathbf{v}_i = \mathbf{R}(\theta) \mathbf{v}(\varphi_i) = \mathbf{R}(\theta) \mathbf{v}(-\text{FOV}/2 + \Delta \cdot i)$,

$$\sum_i^n \mathbf{v}_i \mathbf{v}_i^\top \simeq \frac{1}{\Delta} \mathbf{R}(\theta) \left[\int_{-\text{FOV}/2}^{+\text{FOV}/2} \mathbf{v}(\varphi) \mathbf{v}(\varphi)^\top d\varphi \right] \mathbf{R}(\theta)^\top = \frac{n}{2} \mathbf{I} \quad (27)$$

This is valid if the sampling is dense enough with respect to the bandwidth of f . Analogously $\sum_i \dot{\mathbf{v}}_i \dot{\mathbf{v}}_i^\top \simeq (n/2) \mathbf{I}$. Then finally:

$$E_f\{\mathcal{I}(\mathbf{t})\} = \frac{1}{\sigma^2} \frac{n}{2} \mathbf{I} + \frac{1}{\sigma^2} \mathcal{C} \frac{n}{2} \mathbf{I} = \frac{n}{\sigma^2} \frac{1 + \mathcal{C}}{2} \mathbf{I} \quad (28)$$

c) Derivation of $E_f\{\mathcal{I}(\mathbf{t}, \theta)\}$. By definition:

$$\mathcal{I}(\mathbf{t}, \theta) = \frac{1}{\sigma^2} \sum_i^n \frac{\partial r_i^\top}{\partial \mathbf{t}} \frac{\partial r_i}{\partial \theta} = \frac{1}{\sigma^2} \sum_i^n (\mathbf{v}_i^\top + f'_i \dot{\mathbf{v}}_i^\top) \bar{\rho} f'_i \quad (29)$$

Take the expectation and set $E_f\{f'\} = 0$, to obtain

$$E_f\{\mathcal{I}(\mathbf{t}, \theta)\} = \frac{1}{\sigma^2} \bar{\rho} \mathcal{C} \sum_i^n \dot{\mathbf{v}}_i \quad (30)$$

COVARIANCE OF ICP'S ERRORS COMPARED WITH CRAMÉR–RAO BOUND

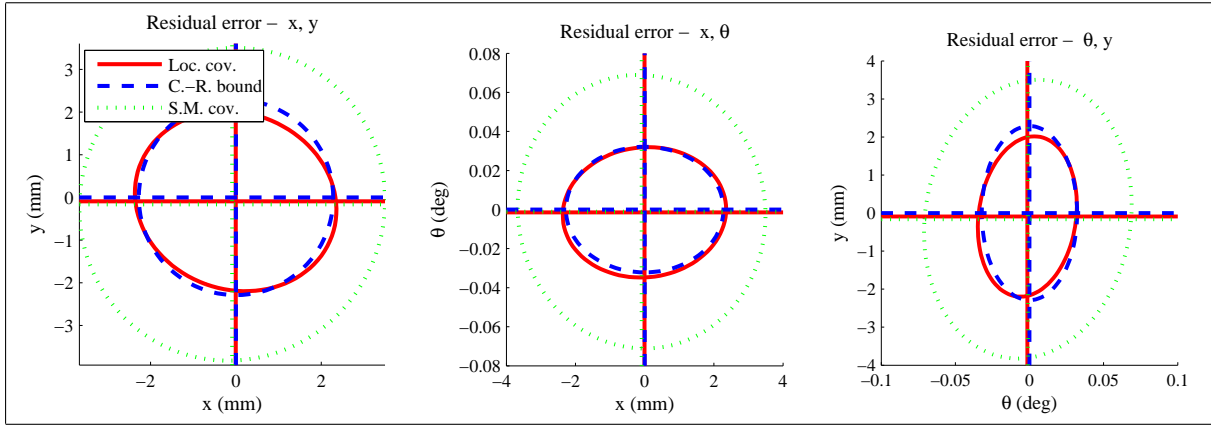
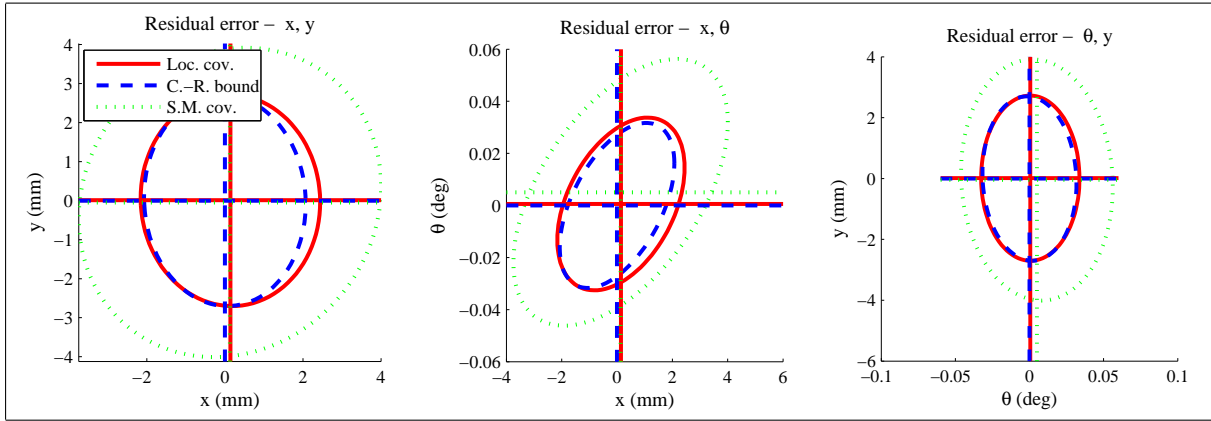
 Symmetric situation: square environment (5m side), FOV = 360°, $\mathbf{x} = (0, 0, 0^\circ)$

 Asymmetric situation: square environment (5m side), FOV = 180°, $\mathbf{x} = (-2m, 2m, 30^\circ)$


Fig. 5. This figures compares the actual error covariance of ICP (continuous line) with the prediction given by the CRB (dashed line): there is an excellent match. However the bound is weak for scan matching (dotted line). The simulated environment is a 5m-side square. For each trial, the sensor scan was simulated adding Gaussian noise with $\sigma = 10mm$. The starting guess was randomly selected according to a Gaussian with mean $(0m, 0m, 0^\circ)$ and $\sigma_x = \sigma_y = 20mm, \sigma_\theta = 0.5^\circ$: this forced good convergence of the algorithm; 200 trials were executed.

For a 360° sensor, $\sum_i \hat{\mathbf{v}}_i \simeq \mathbf{0}$ (for reasons of symmetry), while for a 180° one can approximate the sum with the same procedure as in (27), and obtain $\sum_i \hat{\mathbf{v}}_i \simeq \mathbf{R}(\theta) \begin{bmatrix} 0 & (2n/\pi) \end{bmatrix}^T$.

REFERENCES

- [1] A. Censi, “An accurate closed-form estimate of ICP’s covariance,” in *Proceedings of the IEEE International Conference on Robotics & Automation (ICRA)*, 2007.
- [2] A. Diosi and L. Kleeman, “Uncertainty of line segments extracted from static Sick PLS laser scans,” in *Australasian Conference on Robotics and Automation*, (Brisbane), 2003.
- [3] K. Lingemann, A. Nüchter, J. Hertzberga, and H. Surmann, “High-speed laser localization for mobile robots,” *Robotics and Autonomous Systems*, no. 51, pp. 275–296, 2005.
- [4] G. Casella and R. L. Berger, *Statistical Inference*. Duxbury Press, 1990.
- [5] Z. Zhang, “Iterative point matching for registration of free-form curves,” *International Journal of Computer Vision*, vol. 2, no. 13, pp. 119–152, 1994.
- [6] J. Minguez, F. Lamiroux, and L. Montesano, “Metric-based scan matching algorithms for mobile robot displacement estimation,” *IEEE Transactions on Robotics*, 2006.
- [7] S. Pfister, K. Kriechbaum, S. Roumeliotis, and J. Burdick, “Weighted range sensor matching algorithms for mobile robot displacement estimation,” in *Proceedings of the IEEE International Conference on Robotics & Automation (ICRA)*, 2002.
- [8] G. Grisetti, G. Tipaldi, C. Stachniss, W. Burgard, and D. Nardi, “Speeding-up rao-blackwellized SLAM,” in *Proceedings of the IEEE International Conference on Robotics & Automation (ICRA)*, (Orlando, FL, USA), 2006.
- [9] D. Crisan and A. Doucet, “A survey of convergence results on particle filtering for practitioners,” *IEEE Transactions on Signal Processing*, vol. 50, no. 3, pp. 736–746, 2002.
- [10] T. Tasdizen and R. Whitaker, “Cramer–Rao bounds for nonparametric surface reconstruction from range data,” in *Fourth International Conference on 3D Digital Imaging and Modeling (3DIM)*, 2003.
- [11] J. C. Ye, Y. Bresler, and P. Moulin, “Cramer–Rao bounds for 2-D target shape estimation in nonlinear inverse scattering problems with application to passive radar,” *IEEE Transactions on Antennas and Propagation*, vol. 49, no. 5, pp. 771–783, 2001.
- [12] A. Hero, R. Piramuthu, J. Fessler, and S. Titus, “Minimax emission computed tomography using high-resolution anatomical side information and B-spline models,” *IEEE Transactions on Information Theory*, vol. 45, no. 3, pp. 920–938, 1999.
- [13] J. C. Ye, Y. Bresler, and P. Moulin, “Cramer–Rao bounds for parametric shape estimation in inverse problems,” *IEEE Transactions on Image Processing*, vol. 12, no. 1, pp. 71–84, 2003.
- [14] “The Gaussian Process web site.” <http://www.gaussianprocess.org>.
- [15] A. Elfes, “Using occupancy grids for mobile robot perception and navigation,” *IEEE Computer*, vol. 22, no. 6, 1989.